Pulsed Resonant Charging Power Supply for the Spallation Neutron Source Extraction Kicker PFN System*

R. Saethre[ξ], B. Morris, V. Peplov
Oak Ridge National Laboratory, 9500 Spallation Drive
Oak Ridge, TN, USA

Abstract

The Spallation Neutron Source (SNS) at Oak Ridge National Laboratory uses fourteen pulsed modulators in the extraction system to deflect the proton beam from the accumulation ring to the target. Each individual pulse modulator is a pulse-forming network (PFN) located in a service building external to the ring tunnel. SNS is in the planning and development phase of a proton power upgrade (PPU) to increase the beam energy from 1.0 to 1.3 GeV, and the extraction system is required to provide the same deflection at the higher beam energy. Increasing the magnet current, by charging the PFN to a higher voltage, by 20% will provide the required deflection. The existing capacitor charging power supply is incapable of charging the PFN to higher voltages between the 60 Hz pulses; therefore, a new resonant charging scheme has been developed to charge to the PPU higher voltage within the available time. This paper describes the resonant charging power supply design and presents test results from a prototype operating on a full system test stand.

I. INTRODUCTION

The SNS extraction system [1–3] utilizes fourteen Blumlein PFN modulators to provide pulsed current through fourteen kicker magnets to extract the proton beam from the accumulation ring and direct it to the mercury target. The PPU project will increase the beam energy from 1.0 GeV to 1.3 GeV. This stiffer beam will require a higher integrated magnetic field to fully deflect the proton beam from the accumulation ring. Initial designs included adding two additional magnets operating in conjunction with the existing fourteen magnets. Estimates for this option totaled $4.7M including the cost of the annex vacuum chambers, magnets, cabling, PFN modulators, controls, and diagnostics. An alternative that increases the current in each magnet by 20% was proposed. This can be accomplished by charging the PFN to a higher voltage. The existing capacitor charging power supply is incapable of charging the PFN to higher voltages between the 60 Hz pulses; therefore, a new resonant charging scheme has been developed to charge to the PPU higher voltage within the available time.

II. THEORY

A resonant charging scheme utilizes a capacitor-inductor-capacitor (CLC) circuit, shown in Fig. 1, with a switch to initiate energy transfer from C0 to C1. The initial conditions start with switch S1 open, capacitor C0 charged to voltage V, and C1 discharged. When switch S1 closes, current begins to flow from C0 through L into C1. A series blocking diode is added after the inductor to prevent the current resonating back to C0 and to hold the charge on capacitor C1.

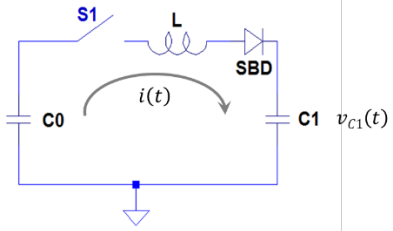

Figure 1. Simple CLC circuit for resonant energy transfer and a series blocking diode (SBD) to hold voltage on C1.

The voltage and current of the charging waveform for capacitor C1 follows Eq. (1) and (2) [4–5].

$$v_{C1}(t) = \frac{V_{C0}}{1+\frac{C1}{C0}} (1 - \cos \omega t) \qquad (1)$$

---

* This manuscript has been authored by UT-Battelle, LLC, under contract DE-AC05-00OR22725 with the US Department of Energy (DOE). The US government retains and the publisher, by accepting the article for publication, acknowledges that the US government retains a nonexclusive, paid-up, irrevocable, worldwide license to publish or reproduce the published form of this manuscript, or allow others to do so, for US government purposes. DOE will provide public access to these results of federally sponsored research in accordance with the DOE Public Access Plan (http://energy.gov/downloads/doe-public-access-plan).

ξ email: saethrerb@ornl.gov

$$i(t) = V_{C0}\sqrt{\left(\frac{C_{eq}}{L}\right)}\,(\sin \omega t), \qquad (2)$$

where $C_{eq} = \frac{C0 \cdot C1}{C0+C1}$.

The resonant frequency is defined by Eq. (3).

$$\omega = \sqrt{\frac{1}{L}\left(\frac{1}{C0}+\frac{1}{C1}\right)} = 2\pi f = \frac{2\pi}{T} \qquad (3)$$

When time t is equal to the resonant half period (τ), $\omega t = \pi, \cos \omega t = -1$, and $v_{C1}(t)$ is at a maximum.

$$v_{max}(\tau) = \frac{2V_{C0}}{1+\frac{C1}{C0}}$$

If capacitor C0 is chosen to be much greater than C1, then the voltage C1 will ring to a maximum of approximately 2x the initial voltage of C0.

For practical components, there is a diminishing return on increasing the value of C0 relative to C1 (Eq. (4) and (5)). If $C0 = 20 \cdot C1$,

$$v_{max}(\tau) \cong 1.9V_{C0} \qquad (4)$$

and

$$\omega \cong \sqrt{\frac{1}{L \cdot C1}} \rightarrow \tau \cong \pi\sqrt{L \cdot C1}\,. \qquad (5)$$

The extraction kicker PFN requires charge voltages up to 45 kV. A voltage of approximately 25 kV would be required when relying on resonant ring-up without a transformer. A 20x step-up pulse transformer lowers the S1 and S2 switch voltage requirements to be compatible with standard off-the-shelf devices.

This scheme is limited by the dc power supply's ability to maintain regulation of the storage capacitor's voltage. A method of regulating the output voltage and allowing loose regulation of the C0 voltage is to add a freewheel diode, FWD, after switch S1 to allow current to continue to flow if switch S1 is opened. C0 is charged to a voltage that will allow maximum output voltages required by the PFN, and an energy calculation is used to open S1 for lower voltages. This allows varying of the C1 voltage without changing the C0 voltage on a pulse-to-pulse basis. The energy calculation is accomplished by measuring the energy in the system (the energy in inductor L plus the energy in C1) and opening switch S1 when there is enough energy in the system to reach the desired final voltage. The regulation is limited by characteristics of the components used in the circuit (e.g., the speed of the S1 switch, the accuracy and repeatability of the energy calculator).

Switch S2 across the inductor L can be used to further improve regulation. If the energy calculation is set to open S1 when there is slightly more energy in inductor L and capacitor C1 than required to reach the final voltage, switch S2 can be closed when the final voltage is achieved shorting the inductor and stopping current flowing to C1. The circuit with the freewheel diode and deque switch is shown in Fig. 2. The sequence of triggering the switches is as follows:

1. S2 is closed, and S1 is open and waits for trigger
2. System receives a trigger
3. S2 is opened, and S1 is closed
4. Energy calculation determines when to open S1
5. C1 voltage is achieved, and S2 is closed
6. PFN is discharged through magnet load
7. System waits for next trigger

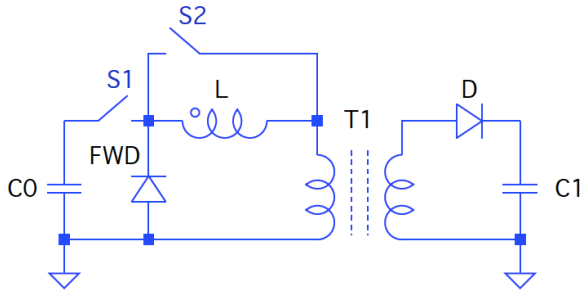

Figure 2. Resonant circuit with a freewheel diode (FWD) and inductor shorting switch (S2) for fine regulation of the final C1voltage. C1 is the equivalent parallel capacitance of the PFN.

A. Energy Calculation

As described earlier, determining when to open switch S1 is accomplished by measuring the energy (current) in the inductor and energy (voltage) stored in the load capacitor, C1. Switch S1 is opened at t_1 when the energy in the inductor, L, plus the energy in capacitor, C1, equals the desired final energy on C1 as calculated in Eq. (6).

$$E_f = E_L(t_1) + E_{C1}(t_1) \qquad (6)$$

Substituting for the inductor and capacitor energy equations and solving for the final voltage:

$$E_f = \frac{1}{2}C1{V_f}^2 = \frac{1}{2}Li^2(t_1) + \frac{1}{2}C1v^2(t_1)$$

$$V_f = \sqrt{\frac{L}{C1}i^2(t_1) + v^2(t_1)}. \qquad (7)$$

Therefore, opening the switch when Eq. (7) is satisfied will result in the desired final voltage on C1 if C0 is charged to a voltage higher than $V_f/(1.9 \cdot N)$ per Eq. (4). Eq. (7) is ideal and neglects magnetizing inductance currents, winding, diode, and switch losses. Opening the switch at a time after Eq. (7) is satisfied will still allow the system to reach the final voltage with regulation controlled by switch S2.

This equation can be realized using digital or analog circuitry. A four-quadrant multiplier/divider chip from

Analog Devices (AD734) [6] was chosen to perform the calculation. This chip can perform analog multiplication, division, squaring, and square root functions to realize Eq. (7) in real time.

B. Component Selection for Resonant Transfer to the Extraction Kicker PFN

Selecting a design point at which the circuit will operate is governed by the transformer step-up ratio, the resonant half period, and the availability of common off-the-shelf components. Use of power electronic switches capable of fast turn on and turn off is desirable to reduce switching losses and errors in the energy calculation. These requirements can be summarized in the following design rules:

- A low transformer ratio requires high primary voltages but has the advantage of lower currents.
- Using a long resonant period requires larger transformer cores to prevent saturation, while a faster period creates higher currents.

A compromise between the competing parameters is shown in Table 1. A transformer ratio of 20x allows selection of 1700 V or 3300 V insulated-gate bipolar transistors (IGBTs) and a storage capacitance of 1300 μF. IGBT peak currents of 1280 A are a concern, but this application operates with a pulse repetition rate of 60 Hz and less than 1% duty. The turn on/off time of these IGBTs are sufficient to meet the regulation requirements.

Table 1. Resonant charging power supply optimized design values.

Item	Value
Total PFN load capacitance, C1	150 nF
PFN voltage range	18–46 kV
Step-up pulse transformer	1:20
dc power supply voltage	1250–1500 V
Storage capacitance, C0	1300 μF
C0 to C1 ratio, referred to same side of transformer	22:1
Resonant half period (τ)	180 μs
Resonant choke inductance, L	56 μH
Transformer peak primary current	1280 Apk
Transformer peak secondary current	64 Apk

C. Extraction Kicker PFN Circuit

The extraction kicker PFN, schematic shown in Fig. 3, consists of 30 stages of capacitors and inductors in a Blumlein configuration. The individual magnets are located in the ring tunnel approximately 100 m from the service building and are connected via two 50-ohm cables in parallel. A high-voltage solid-state switch (S56-12 in Fig. 3) [2] discharges the PFN through the magnet to create the magnetic field required to kick the beam from the accumulation ring.

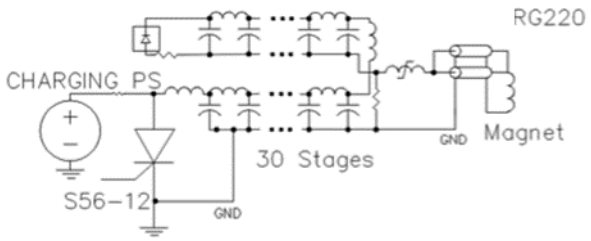

Figure 3. SNS extraction kicker PFN [2] simplified schematic. The new resonant charging power supply is designed to replace the "Charging PS."

D. Circuit Simulations

Results of a simulation are shown in Fig. 4 from a LTSpice® model (Fig. 5) using the component values from Table 1. The transformer's primary and secondary voltage and current waveforms match Eq. (1) and (2). The simulation used 1250 V as the initial C0 voltage, and switch S1 closed at time t_0 = 10 μs. The peak current was 1.28 kA and occurred 90 μs later, which matched the resonant quarter period or τ/2. The simulation did not include an energy calculation to determine when the charge switch opened. It was manually set to open S1 at t_1 = 155 μs and to close the deque switch, S2, at time t_2 = 167 μs. The primary voltage rang up to 2.25 kV or 1.8x the C0 charge voltage. The secondary voltage rang up to 45 kV for a total step-up of 36x. These are lower than the theoretical 1.9x at the primary due to the opening of S1 and closing of S2 prior to full resonance. The waveforms match equations (1–5) above.

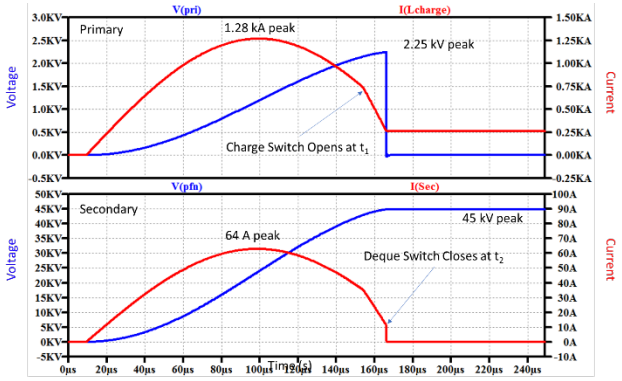

Figure 4. Simulated waveforms using LTSpice®. The upper plot shows the voltage (blue) and current (red) of the primary of the transformer, and the lower plot shows the secondary for a simulated voltage pulse of 45 kV with a charge voltage of 1250 V.

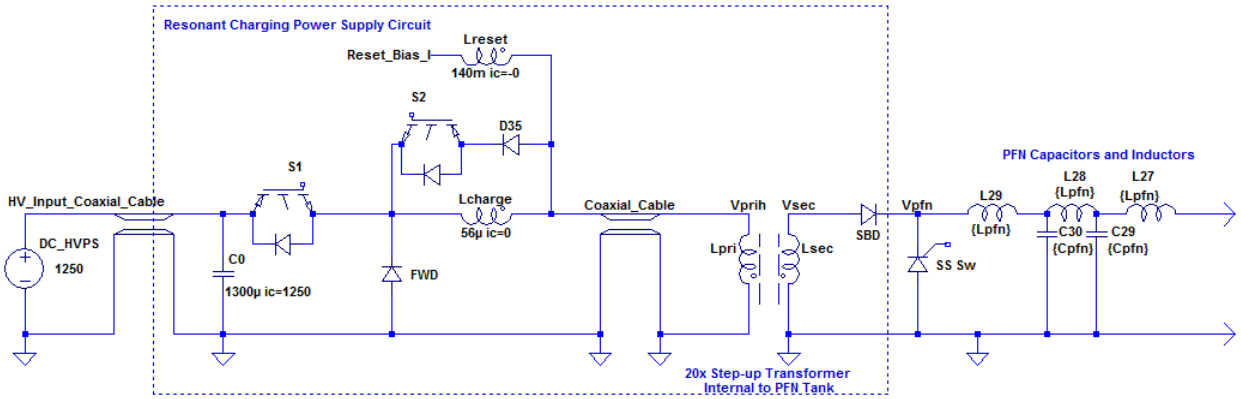

Figure 5. Simplified LTSpice® simulation schematic of the resonant charging power supply circuit (all components within the dotted box.) Only the high-voltage switch and first two stages of the PFN circuit are shown.

E. Development Hardware

A proof-of-concept power supply (Fig. 6) was constructed using the requirements from Table 1 and the component values shown in Fig. 5. A 1700 V IGBT was chosen for S1 and a 3300 V IBGT for S2. S2 is required to block the full output voltage when switch S1 opens and the freewheel diode, FWD, starts conducting, pulling the S2 emitter to a diode drop above ground. The air core inductor was hand-wound to an inductance of 56 μH. Two 1900 V 650 μF capacitors in parallel form capacitor C0. A dc bias current of 10 A is supplied through an isolation inductor to reset the transformer core between pulses. The isolation inductor and 20x step-up pulse transformer were custom-designed and manufactured by Stangenes Industries.

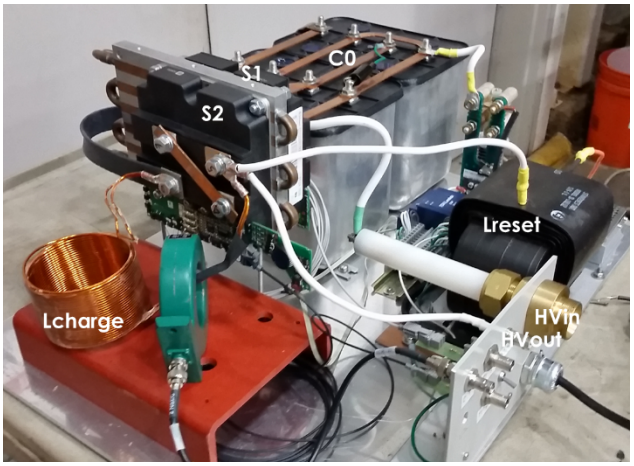

Figure 6. Proof-of-concept resonant charging power supply used to develop a 45kV charging supply.

F. Proof-of-Concept Power Supply Testing

The proof-of-concept power supply was used to verify the system design parameters. With C0 charged to 1 kV, a single pulse from the power supply produced a current waveform with a resonant quarter period (τ/2) of 100 μs, a peak current of 1044 A, and a voltage of 1690 V, as shown in Fig. 7. The peak primary current and resonant quarter period matched the simulation and design equations above. The voltage is slightly lower than 1800 V predicted due to the stray losses in the circuit. The secondary demonstrated a 20x step-up from the primary with a peak voltage of 36 kV shown in Fig. 8. The voltage drooped to 34 kV after switch S2 closed due to the series blocking diode snubber (not shown in the schematic.)

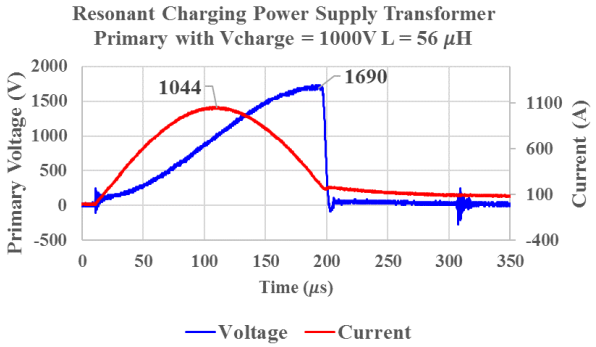

Figure 7. Transformer primary current (red) and voltage (blue) waveforms with a resonant quarter period (τ/2) of 100 μs, a peak current of 1044 A, and voltage of 1690 V.

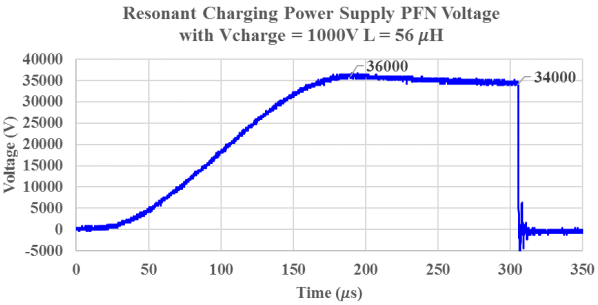

Figure 8. Transformer secondary voltage waveform with a C0 voltage of 1000 V demonstrating a resonant ring-up to 36 kV with a droop to 34 kV.

G. *Solid-State Switch Self-Triggering and Transformer Saturation*

At C0 capacitor voltages above 1100 V, the solid-state switch, SS SW, [2] in the PFN began to self-trigger, causing prefiring before reaching the final PFN voltage required. The red trace in Fig. 9 shows the voltage for a C0 voltage of 1190 V ringing up to 42.4 kV and holding until the solid-state switch is triggered to fire at 310 μs. The blue trace shows the voltage reaching 45.2 kV prior to the solid-state switch self-triggering at 186 v/μs.

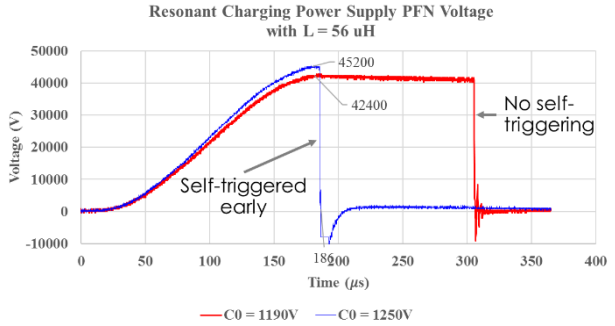

Figure 9. PFN voltages for a C0 charge voltage of 1190 V (red trace) holding off until the PFN is triggered and for 1250 V (blue trace) showing self-triggering at 186 μs.

The manufacturer of the solid-state switch limited the maximum charge rate of the SS SW to 720 V/μs to protect the individual switch modules to ensure all twelve in series turn on at the same time. Increasing the inductance will decrease the charge rate according to Eq. (8) below.

Differentiating Eq. (1) with C0 >> C1 gives the maximum charge rate at $\tau/2$.

$$\frac{dv}{dt}\{V_{C0}(1-\cos\omega t)\} = \omega V_{C0}\sin\omega t = \frac{V}{\sqrt{L\cdot C1}} \quad (8)$$
$$when\ t = \tau\ /\ 2$$

Using Eq. (8) and translating the inductance to the secondary for inductor L (56 μH) will result in a peak charge rate of 776 V/μs at a PFN voltage of 45 kV. Increasing the inductance to 100 μH will reduce the peak charge rate to 581 V/μs. A new inductor was fabricated with an inductance of 100 μH and retested, but the transformer began to saturate at voltages above 34 kV (Fig. 10). The red trace shows the PFN charging to 34 kV and holding until the solid-state switch is triggered, but the primary voltage discharges and rings due to the transformer saturation.

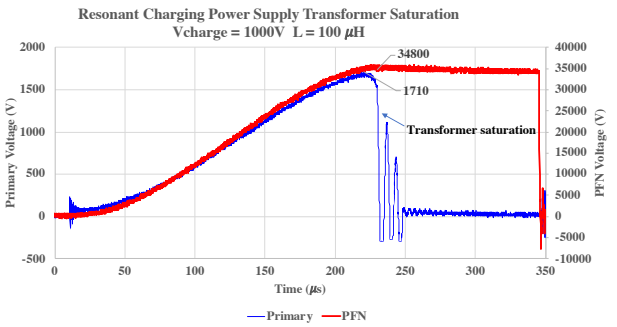

Figure 10. Chart showing the transformer primary voltage (blue trace) saturation at 220 μs and the PFN voltage reaching 34.8 kV and holding until the solid-state switch is triggered.

The integral V·dt, or volt-seconds, applied to the transformer core [7] in the circuit during the pulse is derived from Eq. (1) and Eq. (5) with C0 >> C1:

$$v\tau = \int_0^{\tau} V_{C0}(1-\cos\omega t)\,dt = V_{C0}\pi\sqrt{L\cdot C1}. \quad (9)$$

The volt-seconds of 1st article transformer was designed for 190 mV·s. Increasing the inductance to 100 μH limits the voltage on the primary of the transformer to 1.7 kV or 35 kV on the secondary.

Fig. 11 is a plot of Eq. (8) and (9) for varying inductances and limits of the safe operating area for the transformer (volt-seconds) and the solid-state switch (dV/dt). Any inductance above 43 μH will cause the transformer to saturate, and any inductance below 66 μH will cause the solid-state switch to self-trigger due to excessive dv/dt. There is no safe operating area for this transformer and switch.

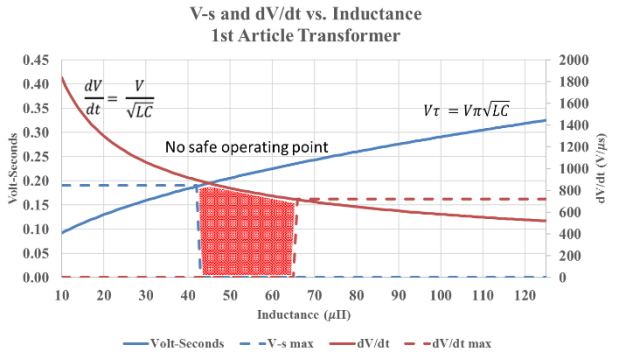

Figure 11. Chart showing the integral V·dt across the transformer and its safe operating area for volt-seconds (blue traces) and for the dv/dt and limitations for the solid-state switch (dV/dt, red traces) for a given choke inductance.

Increasing the core area by 63% allows operating points to overlap with margin at 45 kV as shown in Fig. 12.

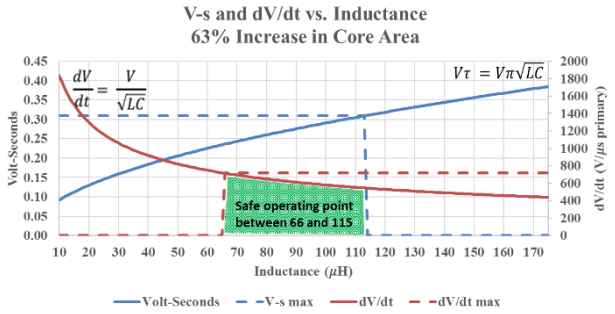

Figure 12. Chart showing the integral V·dt across the transformer and its safe operating area for volt-seconds (blue traces) and for the dv/dt and limitations for the solid-state switch (dV/dt, red traces) for a given choke inductance for an increase of 63% in core area.

A new transformer with 63% more core area was designed and procured, creating a safe operating area for both the transformer and solid-state switch. An inductance of 100 μH was chosen to limit dV/dt to 581 V/μs and the resulting integral V·dt to 290 mV·s. Fig. 13 shows the PFN voltage achieving 43.4 kV with a resonant half period (τ) of 240 μs.

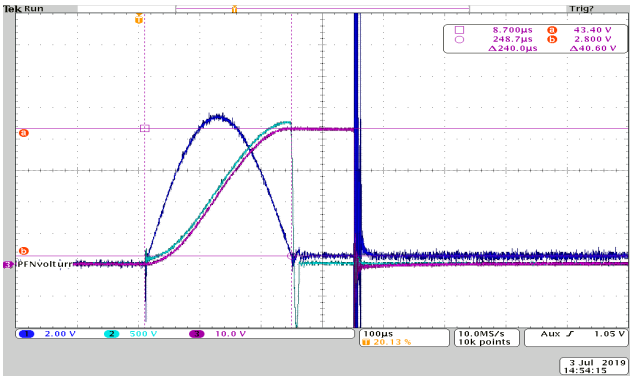

Figure 13. Transformer secondary voltage waveform (Channel 3 magenta 1 kV/V) showing 240 μs resonant half period (τ) charging to 43.4 kV without transformer saturation or solid-state switch self-triggering. Channel 1 (blue) is the primary current (200 A/V) and Channel 2 (light blue) is the primary voltage (1 V/V).

III. SUMMARY

A pulsed resonant charging power supply has been developed for the SNS extraction kicker system that meets the requirements for the PPU project. The new PFN power supply has a faster charge rate, allowing higher voltages than the existing power supplies. The new resonant charging power supply is being developed to a production final design for installation during the PPU project

IV. ACKNOWLEGMENTS

The authors would like to thank Joey Weaver for his efforts during the development process, without which this would not have been possible. This research used resources of the Oak Ridge Leadership Computing Facility, which is a DOE Office of Science User Facility.

V. REFERENCES

[1] R. B. Saethre and M. A. Plum, "SNS proton power upgrade requirements for magnet and kicker systems," in 2017 IEEE 21st International Conference on Pulsed Power (PPC), Brighton, 2017, pp. 1–6. doi: 10.1109/PPC.2017.8291208.

[2] R. Saethre, B. Morris, and H. Sanders, "Thyratron replacement for the Spallation Neutron Source linac extraction kicker PFN system," in 2015 IEEE Pulsed Power Conference (PPC), Austin, TX, 2015, pp. 1–6. doi: 10.1109/PPC.2015.7297034.

[3] C. Pai, et al., "Construction and power test of the extraction kicker magnet for Spallation Neutron Source accumulator ring," in Proceedings of 2005 Particle Accelerator Conference, Knoxville, TN, pp. 3831–3833 (2005)

[4] P. W. Smith, Transient Electronics Pulsed Circuit Technology. West Sussex, England: Wiley & Sons Ltd, 2002.

[5] H. Bluhm, Pulsed Power Systems Principles and Applications. Berlin: Springer, 2006. doi: 10.1007/3-540-34662-7.

[6] Analog Devices, "10 MHz, Four-Quadrant Multiplier/Divider," 2011, AD734 Datasheet, Rev. E https://www.analog.com/media/en/technical-documentation/data-sheets/AD734.pdf.

[7] W. C. Nunnally, "Magnetic switches and circuits," Los Alamos National Laboratory, United States, Tech. Rep. LA-8862-MS, May 1982 https://www.osti.gov/servlets/purl/5256755.